

*Electronic Supplementary Information (ESI) for*

# **Enhanced Visible-Light Photocatalytic Performance of BiOBr/UiO-66(Zr) Composite for Dye Degradation with the Assistance of UiO-66**

Zhou Sha<sup>ab</sup> and Jishan Wu<sup>\*ab</sup>

<sup>a</sup> Department of Chemistry, National University of Singapore, 3 Science Drive 3, Singapore

117543

<sup>b</sup> NUS Environmental Research Institute, National University of Singapore, 5A Engineering

Drive 1, #02-01, Singapore 117411

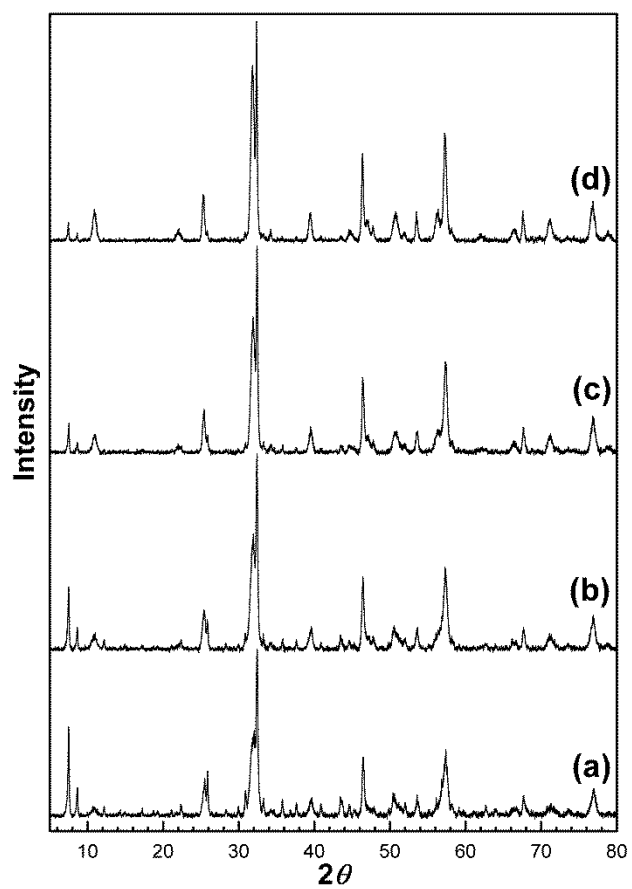


**Fig. S1** XRD patterns of (a) BiOBr/UiO-66-0.5, (b) BiOBr/UiO-66-1, (c) BiOBr/UiO-66-2, and (d) BiOBr/UiO-66-4.

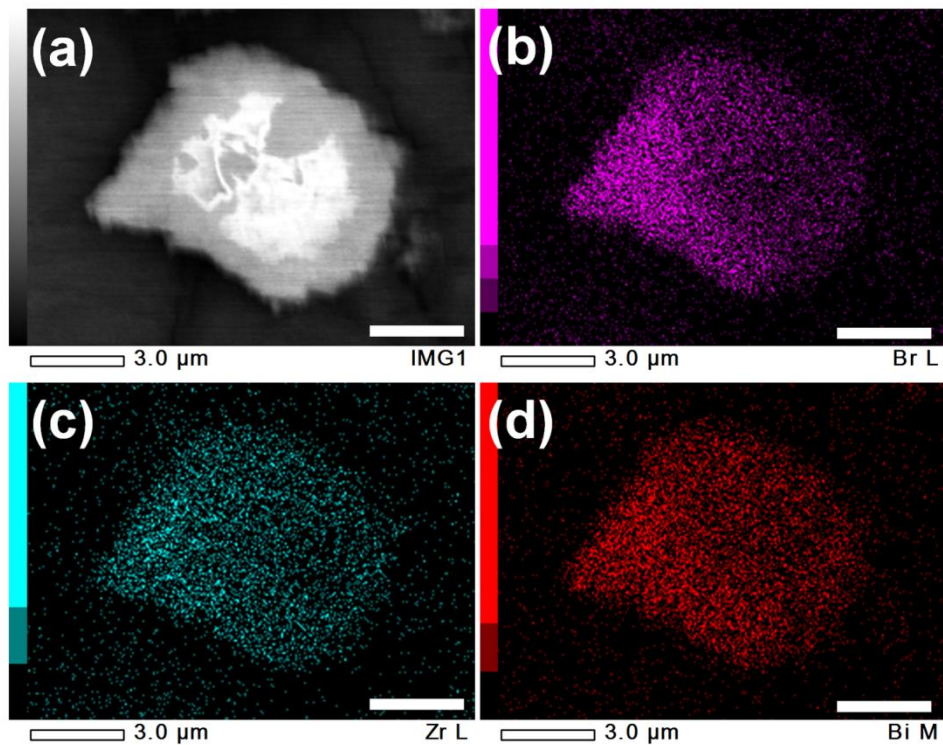


**Fig. S2** (a) SEM image of BiOBr/UiO-66-3, and corresponding EDS elemental mapping images of (b) Br and (c) Zr, and (d) Bi (scale bars are 3  $\mu\text{m}$ ).

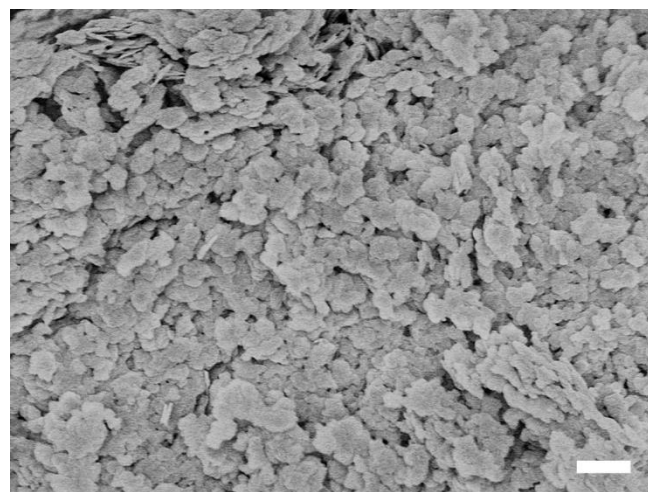


**Fig. S3** SEM image of pristine BiOBr (scale bar is 1  $\mu\text{m}$ ).

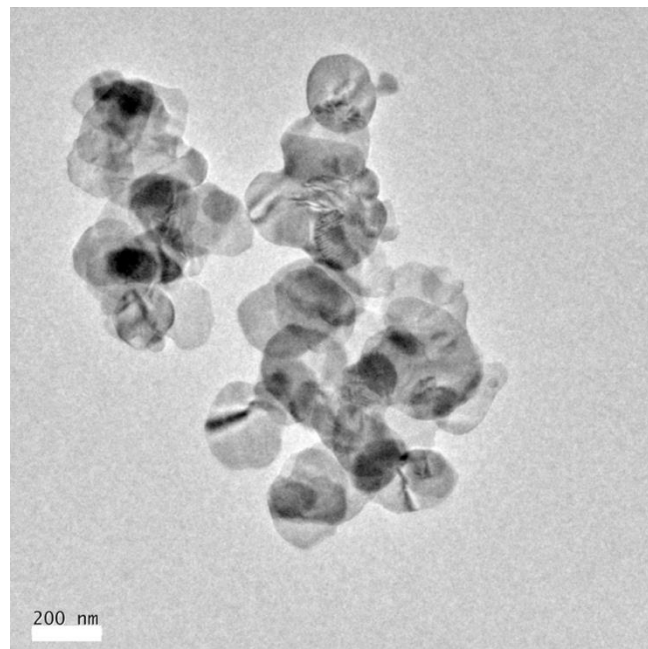


**Fig. S4** TEM image of pristine BiOBr (scale bar is 200 nm).

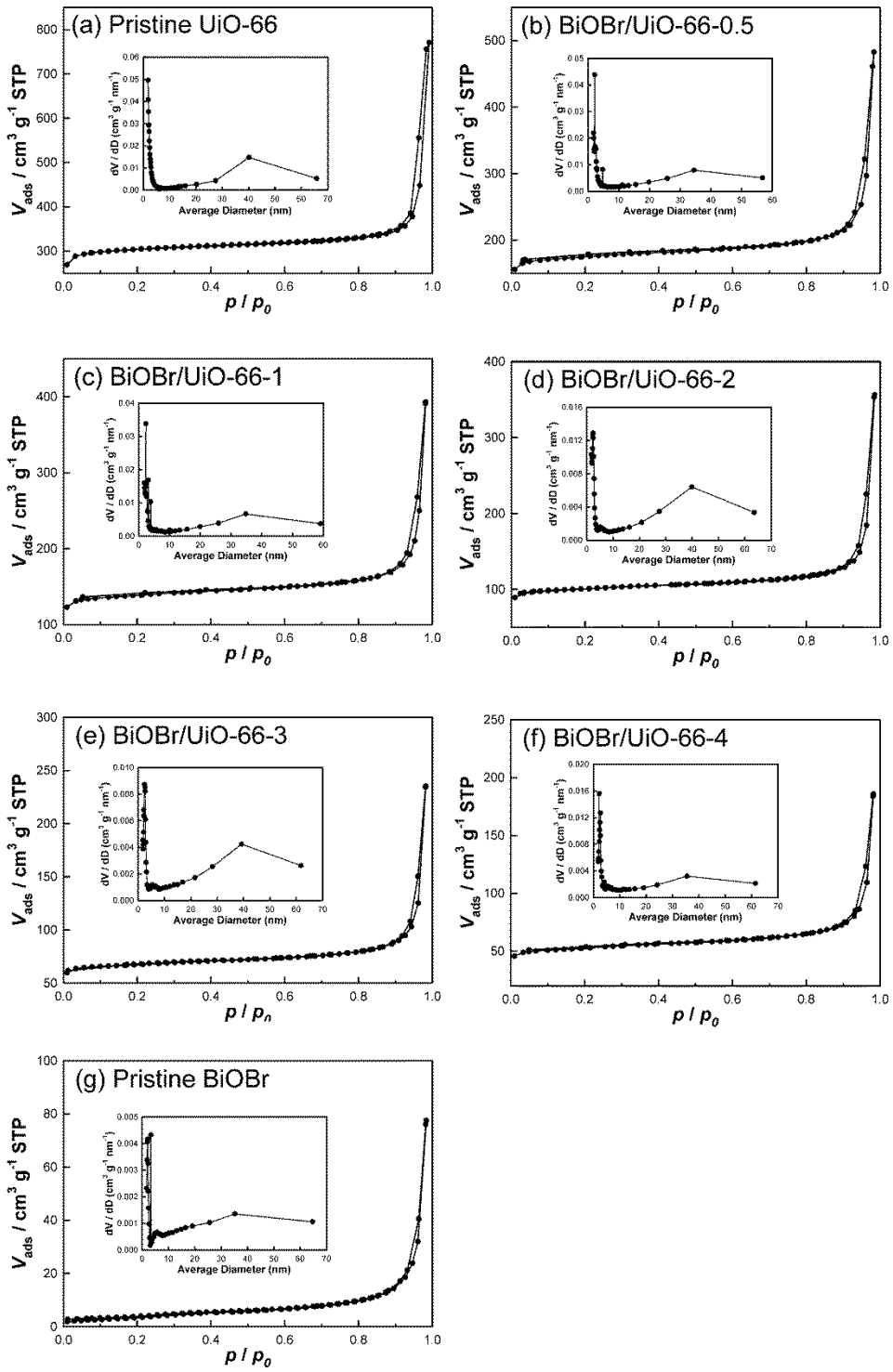


**Fig. S5** Nitrogen adsorption-desorption isotherms and pore size distributions (inset) of (a) pristine UiO-66, (b) BiOBr/UiO-66-0.5, (c) BiOBr/UiO-66-1, (d) BiOBr/UiO-66-2, (e) BiOBr/UiO-66-3, (f) BiOBr/UiO-66-4, and (g) pristine BiOBr.

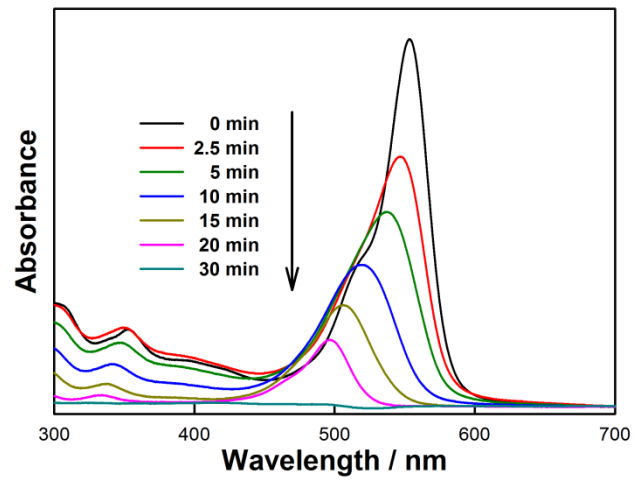


**Fig. S6** UV-Vis spectral changes of RhB solutions as a function of irradiation time in the presence of BiOBr/UiO-66-3.

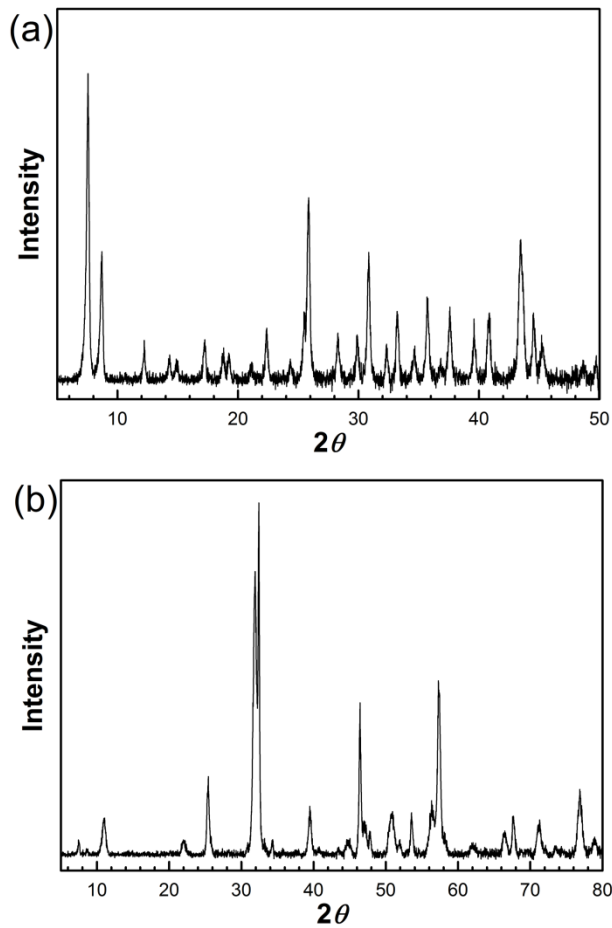


**Fig. S7** XRD patterns of (a) pristine UiO-66-NH<sub>2</sub> and (b) BiOBr/UiO-66-NH<sub>2</sub>-3.

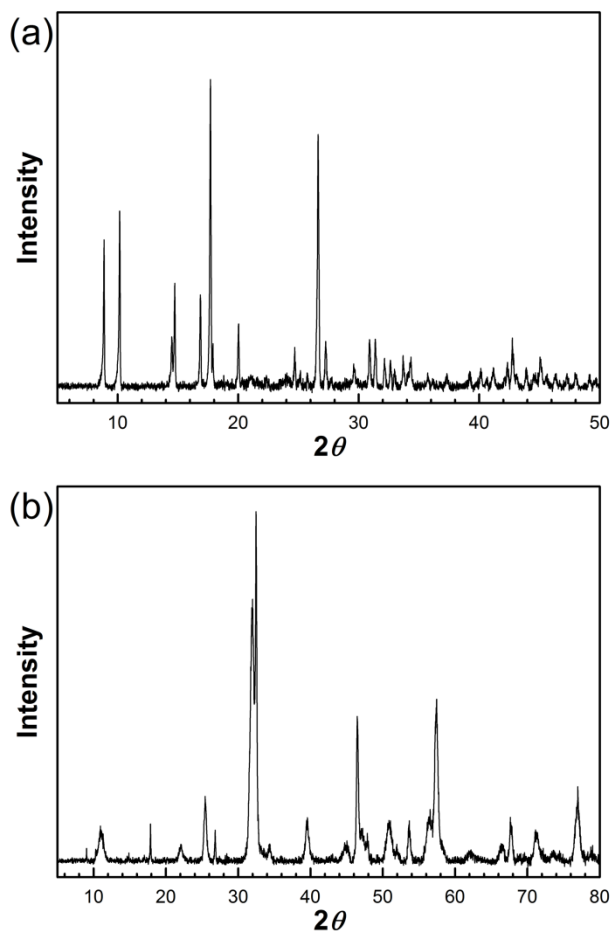


**Fig. S8** XRD patterns of (a) pristine Fe-MIL-53-NH<sub>2</sub> and (b) BiOBr/Fe-MIL-53-NH<sub>2</sub>-3.

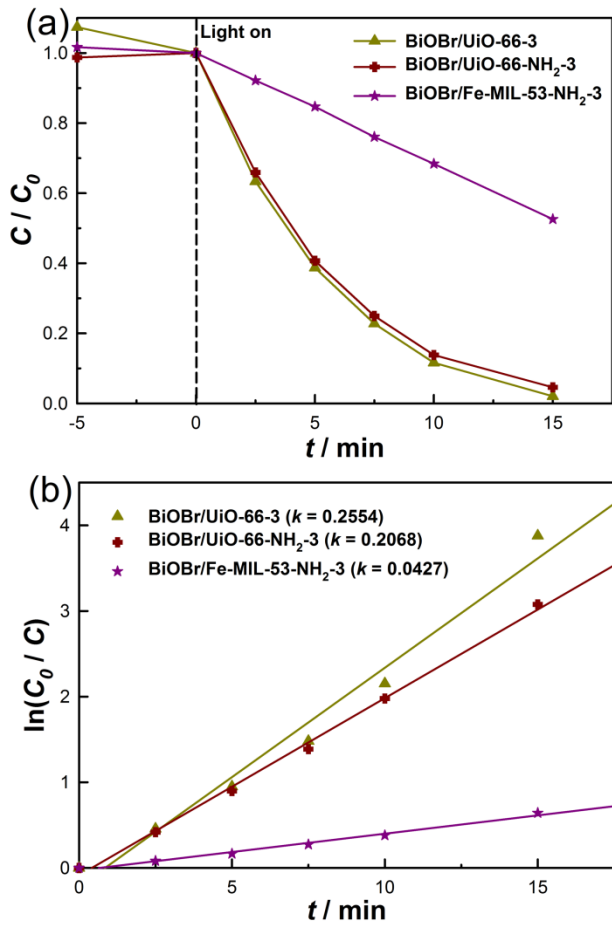


**Fig. S9** Photocatalytic degradation of RhB in the presence of BiOBr/UiO-66-3, BiOBr/UiO-66-NH<sub>2</sub>-3, and BiOBr/Fe-MIL-53-NH<sub>2</sub>-3 under visible-light irradiation. (b) Comparison of the reaction rate constant ( $k$ ) in the presence of BiOBr/UiO-66-3, BiOBr/UiO-66-NH<sub>2</sub>-3, and BiOBr/Fe-MIL-53-NH<sub>2</sub>-3 (assuming that the reactions follow the pseudo-first-order kinetic model).

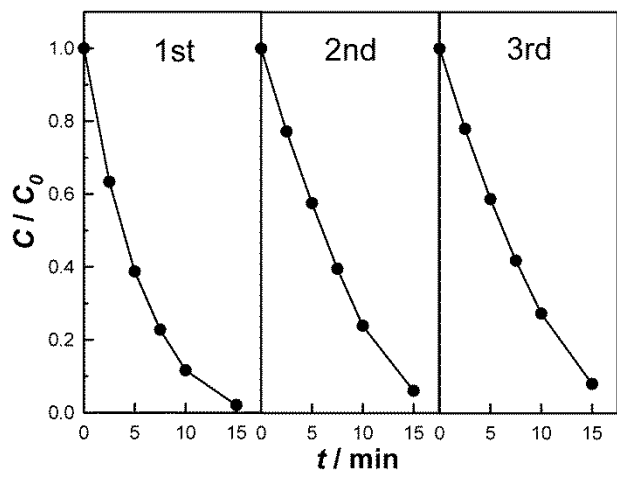


**Fig. S10** Three cycles of the RhB degradation in the presence of BiOBr/UiO-66-3 under visible-light irradiation.

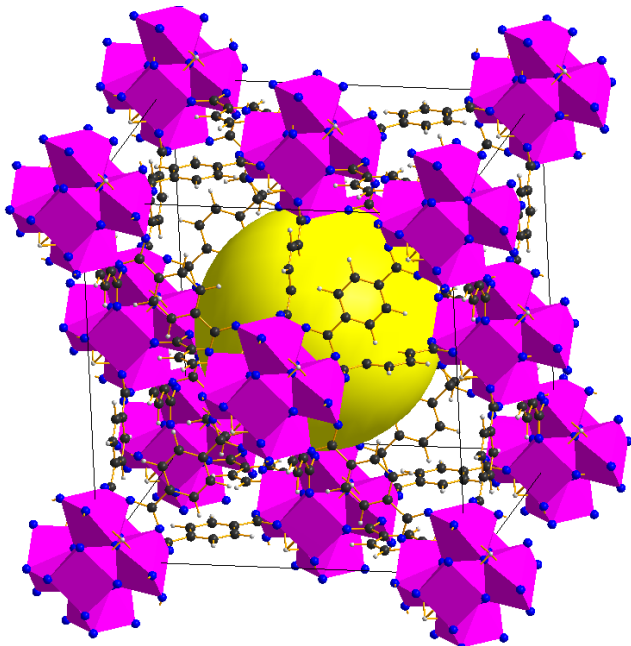


**Fig. S11** Crystal structural illustration of UiO-66. Zirconium, oxygen, carbon, and hydrogen atoms are represented in pink, dark blue, black, and gray, respectively. The large yellow sphere represents the enclosed cavity.

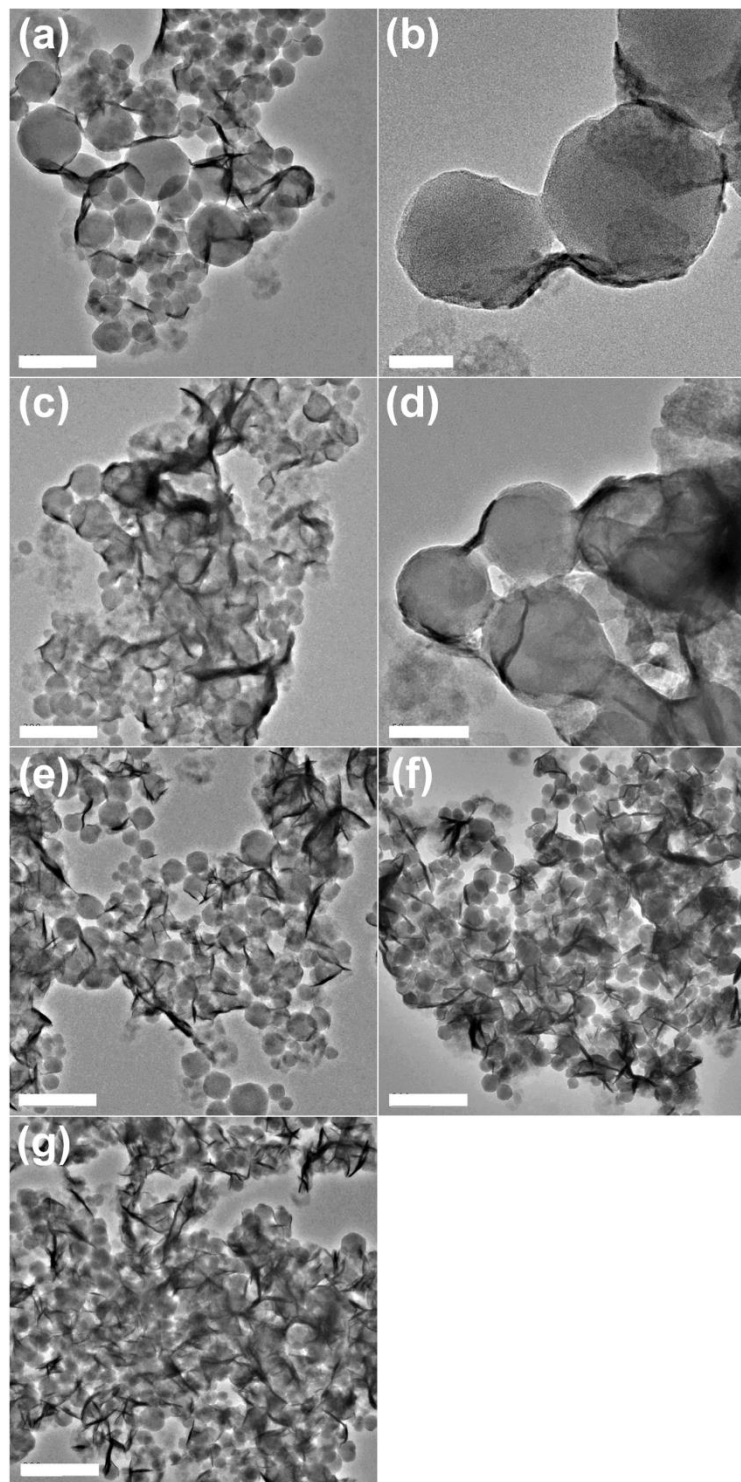


**Fig. S12** TEM images of BiOBr/UiO-66-0.5 sampled at different reaction time: (a, b) 1 min, (c, d) 3 min, (e) 5 min, (f) 10 min, (g) 15 min (scale bars are 200 nm in (a), 50 nm in (b), 300 nm in (c, e), 100 nm in (d), and 400 nm in (f, g)).

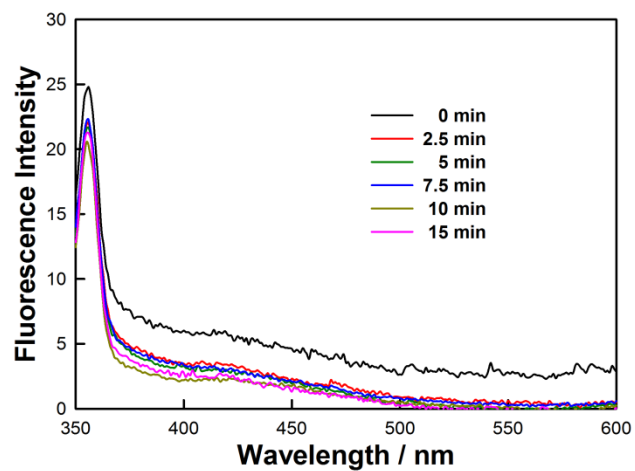


**Fig. S13** Photoluminescence spectral changes with visible-light irradiation time in the presence of BiOBr/UiO-66-3 in a  $5 \times 10^{-4}$  M basic solution of terephthalic acid.